

X-Ray Structural Analyses of Rare Earth Trifluoromethanesulfonate Complexes Bearing Urea Derivatives

Masayoshi Nishiura, Naoko Okano, and Tsuneo Imamoto*

Department of Diversity Science, Graduate School of Science and Technology, Chiba University,
Yayoi-cho, Inage-ku, Chiba 263-8522

(Received March 19, 1999)

X-Ray structural analyses of the rare earth(III) trifluoromethanesulfonates (triflates) with urea derivatives are described. The reactions of anhydrous rare earth triflates with 8 equiv of tetrahydro-2-pyrimidinone (trimethyleneurea (PU)) in methanol give $[M(\text{pu})_8](\text{OTf})_3$ (OTf = triflate) (M = Sm: **1a**; M = Y: **1b**; M = Nd: **1c**; M = Eu: **1d**; M = Gd: **1e**; M = Tb: **1f**; M = Dy: **1g**; M = Ho: **1h**; M = Yb: **1i**), and $[\text{Sc}(\text{pu})_6](\text{OTf})_3$ (**2**). X-Ray crystallographic analyses of these complexes indicate that a pair of PU ligands are interacting with each other through the hydrogen bonds. The reaction of anhydrous samarium(III) triflate with 6 equiv of 1,3-dimethyl-3,4,5,6-tetrahydro-2(1*H*)-pyrimidinone (1,3-dimethyltrimethyleneurea (DMPU)) in tetrahydrofuran (THF) affords $[\text{Sm}(\text{dmpu})_6](\text{OTf})_3$ (**3**) which has a hexa-coordinated octahedral structure. Anhydrous samarium(III) triflate reacts with 5 equiv of 1,3-dimethyl-2-imidazolidinone (DMI) to give $[\text{Sm}(\text{OTf})_2(\text{dmi})_5]\text{OTf}$ (**4**) which has a hepta-coordinated pentagonal bipyramidal structure. Five DMI ligands in **4** coordinate to the samarium atom in a propeller-like fashion.

Rare earth trifluoromethanesulfonates (triflates) are known to behave as characteristic Lewis acids. They are often employed as catalysts in several synthetically useful organic reactions such as aldol reactions, the hetero Diels–Alder reactions, the Friedel Crafts reactions, and esterification of alcohols.^{1,2} Despite their practical utility in organic synthesis, the detailed substrate activation by rare earth triflates has not been well understood in most reactions. Although the coordination of the substrate to the rare earth atoms is a major factor, further understanding of reaction mechanisms, including reactive intermediates, is hampered due to the lack of structural information for rare earth triflate complexes.³ On the other hand, most substrates used in these organic reactions are carbonyl compounds such as ketones, aldehydes, esters, and amides. Therefore, we consider that the determination of the molecular structures of rare earth triflate complexes bearing carbonyl compounds is useful and indispensable for further development of rare earth triflates-promoted organic reactions. This consideration prompted us to carry out the structural study of rare earth triflate complexes with carbonyl compounds by X-ray crystallographic analysis. For this purpose, three urea derivatives: tetrahydro-2-pyrimidinone (trimethyleneurea (PU)), 1,3-dimethyl-3,4,5,6-tetrahydro-2(1*H*)-pyrimidinone (1,3-dimethyltrimethyleneurea (DMPU)), and 1,3-dimethyl-2-imidazolidinone (DMI) were chosen as model carbonyl compounds, because they contain strong electron-donating carbonyl functionalities and are expected to readily form the corresponding rare earth triflate complexes. In this paper, we report the X-ray structural analyses of the rare earth(III) triflate complexes bearing the urea derivatives as ligands.⁴

Experimental

General Methods. All reactions were carried out under argon atmosphere by using Schlenk techniques. THF was distilled from sodium benzophenone ketyl. Methanol was dried over molecular sieves (4A). Chloroform and ethyl acetate were distilled prior to use. Tetrahydro-2-pyrimidinone (trimethyleneurea) was purchased from Tokyo Chemical Industry Co., and used without further purification. 1,3-Dimethyl-2-imidazolidinone and 1,3-dimethyl-3,4,5,6-tetrahydro-2(1*H*)-pyrimidinone were purchased from Wako Pure Chemical Industries Co., dried by stirring with CaH_2 for 24 h, and distilled under reduced pressure. Rare earth oxides were purchased from Nippon Yttrium Co. Trifluoromethanesulfonic acid was supplied from Central Glass Co. Rare earth triflates were prepared by the reaction of rare earth oxides with trifluoromethanesulfonic acid according to the literature.^{2a}

$[\text{Sm}(\text{pu})_8](\text{OTf})_3$ (1a**).** A hot methanol solution (100 cm^3) of tetrahydro-2-pyrimidinone (4.0 g, 40 mmol) was added to a solution of anhydrous samarium(III) triflate (3.0 g, 5 mmol) in MeOH (30 cm^3) at room temperature. After 1 h, the solvent was removed under reduced pressure to give **1** as a white powder (6.2 g, 88%). Mp 206—208 °C. IR (KBr) 3300 m, 1650 s, 1570 m, 1395 m, 1320 w, 1245 m, 1170 w, 1030 m, 760 w, 640 w cm^{-1} . In order to obtain the single crystals for X-ray structural analysis, complex **1** was dissolved in chloroform, and ethyl acetate was slowly layered to give **1** as colorless prisms.

$[\text{Sc}(\text{pu})_6](\text{OTf})_3$ (2**).** A hot methanol solution (5 cm^3) of tetrahydro-2-pyrimidinone (150 mg, 1.5 mmol) was added to a solution of anhydrous samarium(III) triflate (123 mg, 0.25 mmol) in MeOH (1 cm^3) at room temperature. After 1 h, the solvent was removed under reduced pressure to give **1** as a white powder (262 mg, 96%). Mp 185—187 °C. IR (KBr) 3380 m, 3240 m, 1690 m, 1640 s, 1590 m, 1540 w, 1440 w, 1395 w, 1290 w, 1030 w, 640 w cm^{-1} . The single crystals of **2** for X-ray structural analysis were obtained by

the procedure described above.

[Sm(dmpu)₆](OTf)₃ (3). 1,3-Dimethyl-3,4,5,6-tetrahydro-2(1*H*)-pyrimidinone (385 mg, 3 mmol) was added to a solution of anhydrous samarium(III) triflate (299 mg, 0.5 mmol) in THF (5 cm³), whereupon the mixture turned to a white suspension. After 1 h, the solvent was removed under reduced pressure to give **3** as a white powder (580 mg, 85%). Mp 180–182 °C. IR (Nujol[®]) 1590 s, 1548 s, 1420 m, 1270 m, 1150 m, 1080 m, 1030 m, 950 m, 930 w, 750 m, 640 w cm⁻¹. The single crystals for X-ray structural analysis were obtained by recrystallization from THF.

[Sm(OTf)₂(dmi)₅]OTf (4). 1,3-Dimethyl-2-imidazolidinone (285 mg, 2.5 mmol) was added to a solution of anhydrous samarium(III) triflate (299 mg, 0.5 mmol) in THF (5 cm³) with stirring. After 1 h, evaporation of the solvent gave **4** as a white powder (550 mg, 94%). Mp 113–115 °C. IR (Nujol[®]) 1640 m, 1300 m, 1160 w, 1030 m, 780 w, 745 w, 640 w cm⁻¹.

Other PU Coordinated Rare Earth Complexes. These complexes were prepared by the same procedure as that used for preparation of complex **1a**.

[Y(pu)₈](OTf)₃ (1b). Mp 190–196 °C. IR (KBr) 3370 m, 3260 m, 1650 s, 1620 s, 1580 s, 1385 m, 1280 m, 1170 m, 1030 m, 760 w, 640 w cm⁻¹.

[Nd(pu)₈](OTf)₃ (1c). Mp 224–230 °C. IR (KBr) 3300 m, 1650 s, 1570 m, 1395 m, 1320 w, 1245 m, 1170 w, 1030 m, 760 w, 640 w cm⁻¹.

[Eu(pu)₈](OTf)₃ (1d). Mp 209–210 °C. IR (KBr) 3300 m, 1650 s, 1570 m, 1395 m, 1320 w, 1245 m, 1170 w, 1030 m, 760 w, 640 w cm⁻¹.

[Gd(pu)₈](OTf)₃ (1e). Mp 201–202 °C. IR (KBr) 3300 m, 1650 s, 1570 m, 1395 m, 1320 w, 1245 m, 1170 w, 1030 m, 760 w, 640 w cm⁻¹.

[Tb(pu)₈](OTf)₃ (1f). Mp 184–186 °C. IR (KBr) 3300 m, 3080 w, 1650 s, 1570 m, 1440 m, 1395 m, 1315 m, 1245 m, 1170 m, 1030 m, 760 w, 640 w cm⁻¹.

[Dy(pu)₈](OTf)₃ (1g). Mp 172–176 °C. IR (KBr) 3300 m, 1650 s, 1570 m, 1395 m, 1320 w, 1245 m, 1170 m, 1030 m, 760 w,

640 w cm⁻¹.

[Ho(pu)₈](OTf)₃ (1h). Mp 156–160 °C. IR (KBr) 3370 m, 3240 m, 1690 m, 1650 s, 1570 s, 1420 m, 1395 m, 1315 w, 1280 m, 1245 m, 1170 m, 1030 m, 760 w, 640 w cm⁻¹.

[Yb(pu)₈](OTf)₃ (1i). Mp 180–185 °C. IR (KBr) 3370 m, 3260 m, 1695 m, 1650 s, 1620 s, 1570 m, 1440 w, 1390 w, 1315 w, 1280 m, 1250 m, 1170 m, 1030 m, 760 w, 640 w cm⁻¹.

[La(pu)₈](OTf)₃. Mp 223–228 °C. IR (KBr) 3300 m, 3240 m, 1690 m, 1650 s, 1570 m, 1440 w, 1395 m, 1310 w, 1245 m, 1170 w, 1030 m, 760 w, 640 w cm⁻¹.

[Ce(pu)₈](OTf)₃. Mp 224–226 °C. IR (KBr) 3240 m, 3180 m, 1690 s, 1650 s, 1540 m, 1440 m, 1395 m, 1315 m, 1245 w, 1180 w, 1030 w, 760 w, 640 w cm⁻¹.

[Pr(pu)₈](OTf)₃. Mp 234–238 °C. IR (KBr) 3300 m, 1650 s, 1570 m, 1395 m, 1320 w, 1245 m, 1170 w, 1030 m, 760 w, 640 w cm⁻¹.

X-Ray Crystallographic Analyses. The crystals were sealed in glass capillaries. Data collections were performed on an R-AX-ISII diffractometer with graphite-monochromated Mo *K*α radiation. A laser-stimulated fluorescence image plate was used as a two-dimensional area detector. Because of the instability of the crystals, rapid analysis was required. The distance between the crystal and the detector was 85 mm. Thus, 27 frames were recorded at intervals of 6° and each exposure lasted for 5 min (ca. 135 min for the total data collection). Molecular structures of complexes **1a–i** and **4** were solved by direct methods using the program SAPI 91,¹⁸ and complexes **2** and **3** were solved by direct methods using the program SIR 92.¹⁹ Full matrix least-squares refinements were carried out by minimizing the function $\sum w(|F_o| - |F_c|)^2$ where *F*_o and *F*_c were the observed and calculated structure factors. The non-hydrogen atoms were refined anisotropically. Hydrogen atoms were included but not refined. The residual electron densities were of no chemical significance. Crystal data of **1a**, **2**, **3**, and **4** are given in Table 1. Other crystal data of PU coordinated rare earth triflates are described below.

[Sm(OTf)₂(dmi)₅]OTf (4). Disorder was observed in the non-

Table 1. Crystallographic Data for [Sm(pu)₈](OTf)₃ (**1a**), [Sm(pu)₆](OTf)₃ (**2**), [Sm(dmpu)₆](OTf)₃ (**3**), and [Sm(OTf)₂(dmi)₅]OTf (**4**)

Compound	1a	2	3	4
Formula	C ₃₅ H ₆₄ F ₉ N ₁₆ O ₁₇ S ₃ Sm	C ₂₇ H ₄₈ F ₉ N ₁₂ O ₁₅ S ₃ Sc	C ₃₉ H ₇₂ F ₉ N ₁₂ O ₁₅ S ₃ Sm	C ₂₈ H ₅₀ F ₉ N ₁₀ O ₁₄ S ₃ Sm
Fw	1398.55	1092.87	1366.63	1168.33
Crystal system	Triclinic	Monoclinic	Triclinic	Triclinic
Color of crystal	Colorless	Colorless	Colorless	Colorless
Space group	<i>P</i> $\bar{1}$	<i>P</i> 2 ₁ / <i>n</i>	<i>P</i> $\bar{1}$	<i>P</i> $\bar{1}$
<i>a</i> /Å	14.953(3)	8.068(1)	15.594(6)	13.799(7)
<i>b</i> /Å	16.479(4)	21.99(1)	15.636(8)	15.79(1)
<i>c</i> /Å	13.795(3)	25.703(3)	15.569(8)	13.84(2)
α /deg	93.32(1)	90	96.09(4)	109.56(5)
β /deg	113.56(1)	95.17(1)	96.45(3)	116.12(4)
γ /deg	114.62(1)	90	96.48(2)	98.88(8)
<i>V</i> /Å ³	2727(1)	4541(1)	3720(2)	2382(5)
<i>Z</i>	2	4	2	2
<i>T</i> /K	298	173	173	298
<i>D</i> _{calcd} /g cm ⁻³	1.703	1.598	1.220	1.628
μ (Mo <i>K</i> α)/cm ⁻¹	13.05	4.11	9.52	14.69
No. of obsd rflns	6023 (<i>I</i> > 1.00σ(<i>I</i>))	4652 (<i>I</i> > 1.00σ(<i>I</i>))	9325 (<i>I</i> > 3.00σ(<i>I</i>))	6305 (<i>I</i> > 2.00σ(<i>I</i>))
No. of variables	730	604	709	586
<i>R</i> (<i>R</i> _w) ^a	0.061 (0.088)	0.071 (0.089)	0.091 (0.129)	0.071 (0.093)
GOF	1.99	1.78	2.77	2.53

a) $R = \sum ||F_o| - |F_c|| / \sum |F_o|$, $R_w = [\sum w(|F_o| - |F_c|)^2 / \sum wF_o^2]^{1/2}$.

coordinated triflate anion.

[Y(pu)₈](OTf)₃ (1b). Colorless crystal. Crystal data: formula C₃₅H₆₄F₉N₁₆O₁₇S₃Y, formula weight 1337.06, triclinic, space group *P* $\bar{1}$ (No. 2), *a* = 14.840(4), *b* = 16.581(3), *c* = 13.801(6) Å, α = 93.86(2)°, β = 113.45(2)°, γ = 114.29(1)°, *V* = 2729(1) Å³, *Z* = 2, *D*_{calcd} = 1.627 g cm⁻³, No. of observed reflections 5464 (*I* > 1.0σ(*I*)), No. of variables 730, *R* = 0.065, *R*_w = 0.074.

[Nd(pu)₈](OTf)₃ (1c). Pale purple crystal. Crystal data: formula C₃₅H₆₄F₉N₁₆NdO₁₇S₃, formula weight 1392.39, triclinic, space group *P* $\bar{1}$ (No. 2), *a* = 14.975(3), *b* = 16.484(6), *c* = 13.793(3) Å, α = 93.33(3)°, β = 113.58(2)°, γ = 114.38(2)°, *V* = 2738(1) Å³, *Z* = 2, *D*_{calcd} = 1.688 g cm⁻³, No. of observed reflections 5994 (*I* > 1.0σ(*I*)), No. of variables 730, *R* = 0.055, *R*_w = 0.079.

[Eu(pu)₈](OTf)₃ (1d). Colorless crystal. Crystal data: formula C₃₅H₆₄EuF₉N₁₆O₁₇S₃, formula weight 1400.11, triclinic, space group *P* $\bar{1}$ (No. 2), *a* = 14.833(3), *b* = 16.509(2), *c* = 13.675(4) Å, α = 93.54(1)°, β = 113.15(1)°, γ = 114.56(1)°, *V* = 2697(1) Å³, *Z* = 2, *D*_{calcd} = 1.724 g cm⁻³, No. of observed reflections 5725 (*I* > 1.0σ(*I*)), No. of variables 730, *R* = 0.050, *R*_w = 0.064.

[Gd(pu)₈](OTf)₃ (1e). Colorless crystal. Crystal data: formula C₃₅H₆₄F₉GdN₁₆O₁₇S₃, formula weight 1405.40, triclinic, space group *P* $\bar{1}$ (No. 2), *a* = 14.890(6), *b* = 16.559(6), *c* = 13.798(6) Å, α = 93.52(3)°, β = 113.80(3)°, γ = 114.25(2)°, *V* = 2730(2) Å³, *Z* = 2, *D*_{calcd} = 1.709 g cm⁻³, No. of observed reflections 6011 (*I* > 1.0σ(*I*)), No. of variables 730, *R* = 0.058, *R*_w = 0.083.

[Tb(pu)₈](OTf)₃ (1f). Colorless crystal. Crystal data: formula C₃₅H₆₄F₉N₁₆O₁₇S₃Tb, formula weight 1407.08, triclinic, space group *P* $\bar{1}$ (No. 2), *a* = 14.844(7), *b* = 16.561(4), *c* = 13.769(4) Å, α = 93.69(2)°, β = 113.33(2)°, γ = 114.46(2)°, *V* = 2721(2) Å³, *Z* = 2, *D*_{calcd} = 1.717 g cm⁻³, No. of observed reflections 5970 (*I* > 1.0σ(*I*)), No. of variables 730, *R* = 0.048, *R*_w = 0.065.

[Dy(pu)₈](OTf)₃ (1g). Colorless crystal. Crystal data: formula C₃₅H₆₄DyF₉N₁₆O₁₇S₃, formula weight 1410.65, triclinic, space group *P* $\bar{1}$ (No. 2), *a* = 14.881(5), *b* = 16.524(6), *c* = 13.805(2) Å, α = 93.64(3)°, β = 113.54(2)°, γ = 114.41(3)°, *V* = 2725(2) Å³, *Z* = 2, *D*_{calcd} = 1.719 g cm⁻³, No. of observed reflections 5872 (*I* > 1.0σ(*I*)), No. of variables 730, *R* = 0.056, *R*_w = 0.083.

[Ho(pu)₈](OTf)₃ (1h). Colorless crystal. Crystal data: formula C₃₅H₆₄F₉HoN₁₆O₁₇S₃, formula weight 1413.08, triclinic, space group *P* $\bar{1}$ (No. 2), *a* = 14.858(5), *b* = 17.024(5), *c* = 13.755(2) Å, α = 113.68(2)°, β = 113.45(3)°, γ = 98.41(2)°, *V* = 2722(2) Å³, *Z* = 2, *D*_{calcd} = 1.724 g cm⁻³, No. of observed reflections 6054 (*I* > 1.0σ(*I*)), No. of variables 730, *R* = 0.054, *R*_w = 0.076.

[Yb(pu)₈](OTf)₃ (1i). Colorless crystal. Crystal data: formula C₃₅H₆₄F₉N₁₆O₁₇S₃Yb, formula weight 1421.19, triclinic, space group *P* $\bar{1}$ (No. 2), *a* = 14.893(6), *b* = 16.550(4), *c* = 13.791(3) Å, α = 93.64(2)°, β = 113.49(2)°, γ = 114.29(2)°, *V* = 2734(1) Å³, *Z* = 2, *D*_{calcd} = 1.726 g cm⁻³, No. of observed reflections 6106 (*I* > 1.0σ(*I*)), No. of variables 730, *R* = 0.064, *R*_w = 0.094.

[La(pu)₈](OTf)₃. Colorless crystal. Crystal data: formula C₃₅H₆₄F₉LaN₁₆O₁₇S₃, formula weight 1387.06, triclinic, space group *P* $\bar{1}$ (No. 2), *a* = 15.028(7), *b* = 16.263(4), *c* = 13.156(8) Å, α = 89.63(4)°, β = 115.98(4)°, γ = 72.11(3)°, *V* = 2712(2) Å³, *Z* = 2, *D*_{calcd} = 1.698 g cm⁻³. The disorder was observed in ligands and triflate anions. Only the crystal parameters could be determined.

[Ce(pu)₈](OTf)₃. Colorless crystal. Crystal data: formula C₃₅H₆₄CeF₉N₁₆O₁₇S₃, formula weight 1388.27, triclinic, space group *P* $\bar{1}$ (No. 2), *a* = 15.004(5), *b* = 16.27(1), *c* = 13.173(2) Å, α = 90.08(3)°, β = 116.12(2)°, γ = 72.26(4)°, *V* = 2716(1) Å³, *Z* = 2, *D*_{calcd} = 1.697 g cm⁻³. The disorder was observed in ligands and triflate anions.

[Pr(pu)₈](OTf)₃. Pale green crystal. Crystal data: formula C₃₅H₆₄F₉N₁₆O₁₇PrS₃, formula weight 1389.06, triclinic, space group *P* $\bar{1}$ (No. 2), *a* = 15.167(5), *b* = 16.569(5), *c* = 13.353(4) Å, α = 89.93(2)°, β = 116.11(2)°, γ = 72.00(2)°, *V* = 2828(2) Å³, *Z* = 2, *D*_{calcd} = 1.631 g cm⁻³, No. of observed reflections 6088 (*I* > 1.0σ(*I*)), No. of variables 700, *R* = 0.090, *R*_w = 0.125. Some disorder was observed in one of the PU ligands.

Results and Discussion

[M(pu)₈](OTf)₃ (M = Sm: 1a; M = Y: 1b; M = Nd: 1c; M = Eu: 1d; M = Gd: 1e; M = Tb: 1f; M = Dy: 1g; M = Ho: 1h; M = Yb: 1i). We reported previously that the tetrad effect was observed in the coordination bonds of hexamethylphosphoramide (HMPA)-coordinated rare earth triflates.^{3e} In order to confirm the generality of this effect, a series of PU-coordinated rare earth(III) triflates, except promethium, were synthesized by the reactions of anhydrous rare earth(III) triflates with 8 equiv of PU in methanol. The resultant complexes were recrystallized from a mixed solvent of chloroform and ethyl acetate. We tried to determine all the molecular structures; however, in the cases of La, Ce, and Pr complexes, the X-ray structural analyses were not satisfactorily carried out because of the disorder of ligands and triflate anions. Furthermore, single crystals of Er, Tm, and Lu complexes could not be obtained. The other molecular structures of rare earth (Sc, Y, Nd, Sm, Eu, Gd, Tb, Dy, Ho, Yb) complexes were successfully characterized. The ORTEP drawing of [Sm(pu)₈](OTf)₃ (1a) is shown in Fig. 1 as a representative example. The selected bond lengths and angles of 1a are given in Table 2. The central samarium atom is coordinated by eight PU molecules to form a square antiprism geometry. The average bond length (2.426(4) Å) of Sm–O in 1a is shorter than those of Sm–O (THF) in (C₅Me₅)₂Sm(biphenyl-2,2'-diyl ketyl)(thf) (2.519(8) Å)⁵ and Sm–O (THF) in Sm(OSiPh₃)₃(thf)₃·THF (2.529(2) Å),⁶ but is longer than that of Sm–O (HMPA) in [Sm(OTf)₂(hmpa)₄](OTf)·CHCl₃ (2.259(4) Å),^{3f} although the ionic radius of the

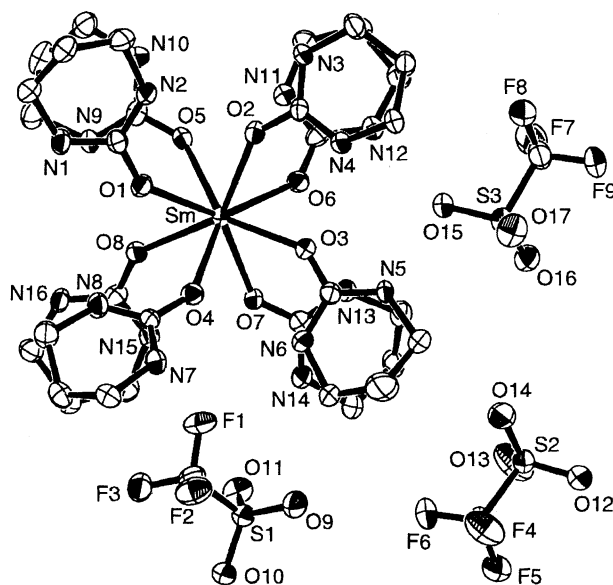


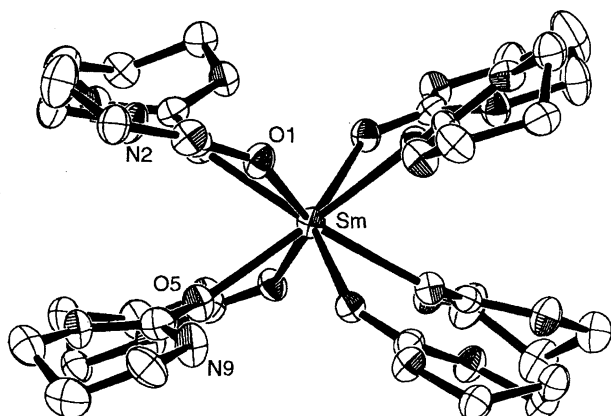
Fig. 1. ORTEP drawing of [Sm(pu)₈](OTf)₃ (1a).

Table 2. Selected Bond Lengths (Å) and Angles (deg) for [M(pu)₈](OTf)₃ (M = Sm: **1a**; M = Y: **1b**; M = Nd: **1c**; M = Eu: **1d**; M = Gd: **1e**; M = Tb: **1f**; M = Dy: **1g**; M = Ho: **1h**; M = Yb: **1i**)

[Sm(pu)₈](OTf)₃ (1a)							
Sm–O(1)	2.409(4)	Sm–O(2)	2.409(4)	Sm–O(3)	2.461(4)		
Sm–O(4)	2.442(4)	Sm–O(5)	2.408(4)	Sm–O(6)	2.409(4)		
Sm–O(7)	2.432(4)	Sm–O(8)	2.441(4)				
O(1)···N(8)	3.018(8)	O(1)···N(9)	3.37(1)	O(2)···N(2)	2.85(1)		
O(3)···N(4)	2.755(8)	O(3)···N(13)	3.163(7)	O(4)···N(6)	2.87(1)		
O(5)···N(2)	3.441(8)	O(5)···N(11)	2.798(7)	O(6)···N(13)	2.84(1)		
O(7)···N(6)	3.272(9)	O(7)···N(15)	2.781(9)	O(8)···N(8)	3.087(6)		
O(8)···N(9)	2.88(1)	O(15)···N(5)	3.138(6)	O(15)···N(12)	2.93(1)		
O(15)···N(13)	3.36(1)	F(1)···N(14)	3.380(6)	F(1)···N(15)	3.35(1)		
F(2)···N(7)	3.36(1)						
O(1)–Sm–O(2)	76.0(1)	O(1)–Sm–O(3)	118.1(1)	O(1)–Sm–O(4)	71.6(1)		
O(1)–Sm–O(5)	75.8(2)	O(1)–Sm–O(6)	142.7(1)	O(1)–Sm–O(7)	140.2(1)		
O(1)–Sm–O(8)	73.9(1)	Sm–O(1)–C(1)	140.8(5)	Sm–O(2)–C(5)	142.1(4)		
Sm–O(3)–C(9)	141.5(4)	Sm–O(4)–C(13)	142.0(5)	Sm–O(5)–C(17)	141.5(5)		
Sm–O(6)–C(21)	140.9(4)	Sm–O(7)–C(25)	138.9(4)	Sm–O(8)–C(29)	142.5(4)		
[Y(pu)₈](OTf)₃ (1b)							
Y–O(1)	2.346(4)	Y–O(2)	2.364(4)	Y–O(3)	2.393(4)	Y–O(4)	2.341(4)
Y–O(5)	2.394(4)	Y–O(6)	2.380(4)	Y–O(7)	2.352(4)	Y–O(8)	2.367(4)
[Nd(pu)₈](OTf)₃ (1c)							
Nd–O(1)	2.439(4)	Nd–O(2)	2.451(4)	Nd–O(3)	2.473(4)	Nd–O(4)	2.479(4)
Nd–O(5)	2.438(4)	Nd–O(6)	2.425(4)	Nd–O(7)	2.459(4)	Nd–O(8)	2.458(4)
[Eu(pu)₈](OTf)₃ (1d)							
Eu–O(1)	2.385(4)	Eu–O(2)	2.406(4)	Eu–O(3)	2.423(4)	Eu–O(4)	2.381(4)
Eu–O(5)	2.434(4)	Eu–O(6)	2.430(4)	Eu–O(7)	2.389(4)	Eu–O(8)	2.396(4)
[Gd(pu)₈](OTf)₃ (1e)							
Gd–O(1)	2.365(4)	Gd–O(2)	2.406(4)	Gd–O(3)	2.412(4)	Gd–O(4)	2.384(4)
Gd–O(5)	2.426(4)	Gd–O(6)	2.411(4)	Gd–O(7)	2.391(4)	Gd–O(8)	2.393(4)
[Tb(pu)₈](OTf)₃ (1f)							
Tb–O(1)	2.368(3)	Tb–O(2)	2.394(3)	Tb–O(3)	2.405(4)	Tb–O(4)	2.370(3)
Tb–O(5)	2.420(3)	Tb–O(6)	2.404(3)	Tb–O(7)	2.368(3)	Tb–O(8)	2.386(3)
[Dy(pu)₈](OTf)₃ (1g)							
Dy–O(1)	2.417(4)	Dy–O(2)	2.381(4)	Dy–O(3)	2.364(4)	Dy–O(4)	2.387(4)
Dy–O(5)	2.381(4)	Dy–O(6)	2.352(4)	Dy–O(7)	2.363(4)	Dy–O(8)	2.396(4)
[Ho(pu)₈](OTf)₃ (1h)							
Ho–O(1)	2.381(4)	Ho–O(2)	2.346(4)	Ho–O(3)	2.357(4)	Ho–O(4)	2.394(4)
Ho–O(5)	2.383(4)	Ho–O(6)	2.337(4)	Ho–O(7)	2.334(4)	Ho–O(8)	2.372(3)
[Yb(pu)₈](OTf)₃ (1i)							
Yb–O(1)	2.373(4)	Yb–O(2)	2.411(4)	Yb–O(3)	2.408(4)	Yb–O(4)	2.380(4)
Yb–O(5)	2.429(4)	Yb–O(6)	2.423(4)	Yb–O(7)	2.383(4)	Yb–O(8)	2.392(3)

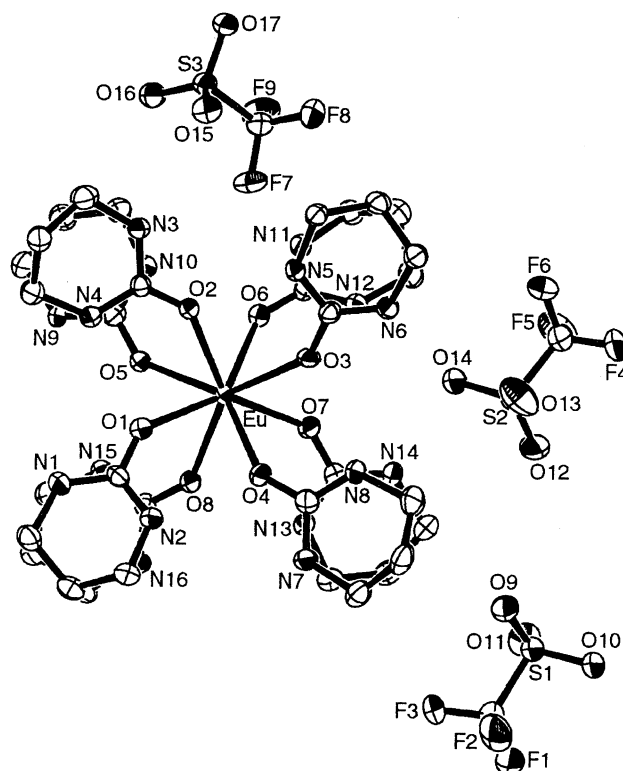
hexa-coordinated samarium ion is 0.12 Å smaller than that of octa-coordinated samarium ion.⁷ These results suggest that the electron-donating ability of PU ligand is stronger than that of THF, but is weaker than that of HMPA ligand. This complex shows a unique coordination form, such that a pair of PU ligands overlap each other. Figure 2 shows the side view of complex **1a**. The unique coordination fashion is mainly attributable to the hydrogen bonding interac-

tion between the upper ligands and lower ligands: O1···N9 (3.37(1) Å) and O5···N2 (3.441(8) Å). The average bond angle (141.3(5)°) of Sm–O–C (carbonyl carbon) is apparently smaller than those of the urea derivative coordinated samarium complexes (discussed below) [Sm(dmpu)₆](OTf)₃ (**2**) (159.1(7)°), [Sm(OTf)₂(dmi)₅](OTf) (**3**) (167.5(7)°), and also smaller than those of the other lanthanide complexes bearing neutral oxygen donor ligands: Sm–O–P

Fig. 2. Side view of $[\text{Sm}(\text{pu})_8](\text{OTf})_3$ (**1a**).

of $[\text{Sm}(\text{Otf})_2(\text{hmpa})_4]\text{Otf}\cdot\text{CHCl}_3$ (av. $171.8(3)^\circ$),^{3f} La–O–P of $[\text{La}\{\text{N}(\text{SiMe}_3)_2\}_3(\text{Ph}_3\text{PO})]$ ($174.6(9)^\circ$),⁸ Sm–O–P of *cis*- and *trans*- $[(\text{C}_5\text{Me}_5)_2(\text{Ph}_3\text{PO})\text{Sm}]_2(\mu\text{-OCH=CHO})$ (av. $168.2(7)^\circ$ and $160.9(5)^\circ$ respectively),⁹ and Y–O–C of $\text{YCl}_3(\varepsilon\text{-caprolactone})_3$ (av. $154.8(2)^\circ$).¹⁰ This narrow bond angle is attributable to the hydrogen bonds such as $\text{O1}\cdots\text{N8}$ ($3.018(8)$ Å) and $\text{O3}\cdots\text{N4}$ ($2.755(8)$ Å) among adjacent ligands. It is noted that these hydrogen bonds are a significant factor to constitute the characteristic molecular structures observed in these PU-coordinated rare earth complexes. Three triflate anions in complex **1a** are not coordinated to the samarium atom, thereby making the complex tricationic, indicating that the PU ligand is a strong oxygen-donor ligand. The triflate anions exist in the outer sphere through the hydrogen bonds between the nitrogen atoms of PU and the oxygen or fluorine atoms such as $\text{O15}\cdots\text{N12}$ ($2.93(1)$ Å) and $\text{F1}\cdots\text{N14}$ ($3.380(6)$ Å).

The other lanthanide complexes with PU ligands also form an octa-coordinated square antiprism structure, as shown in $[\text{Eu}(\text{pu})_8](\text{OTf})_3$ (**1d**) (Fig. 3). However, the positions of the three triflate anions are different from those of **1a**. A similar structure is observed in the yttrium complex due to the similarity of the ionic radius between the yttrium and holmium ion.⁷ The average bond distance ($2.367(4)$ Å) (Table 2) of Y–O bonds in **1b** is shorter than that ($2.450(6)$ Å) of Y–O (carbonyl oxygen) bonds in $[\text{Y}_2(\text{NO}_3)_6\text{L}_3]\cdot 2\text{MeCN}$ ($\text{L} = N,N'$ -*o*-phenylenedimethylenebis(pyridin-2-one)).¹¹ The average coordination bond ($2.453(4)$ Å) (Table 2) of the neodymium complex (**1c**) is longer than those of Nd–O (HMPA) bonds in $[\text{NdCl}(\text{hmpa})_5](\text{PF}_6)_2$ ($2.35(2)$ Å)¹² and Nd–O (phosphine oxide) bonds in $\text{NdL}_2(\text{NO}_3)_3(\text{H}_2\text{O})$ [$\text{L} = (i\text{PrO})_2\text{P}(\text{O})\text{C}(\text{Et})\text{NOH}$] ($2.406(4)$ Å),¹³ but is nearly equal to that of Nd–O bonds of the tricationic unit in the neodymium complex $[\text{Nd}(\varepsilon\text{-caprolactone})]^{3+}[\text{Cl}_3\text{Nd}(\mu\text{-Cl})_3\text{NdCl}_3]^{3-}$ ($2.46(5)$ Å).¹⁴ The average bond distance ($2.406(4)$ Å) (Table 2) of Eu–O bonds in **1d** is nearly equal to that ($2.384(5)$ – $2.435(5)$ Å) of Eu–O (dmf) bonds in $(\text{dmf})_8\text{Eu}_2\text{Ni}(\text{NCO})$ ($\text{dmf} = N,N$ -dimethylformamide).¹⁵ The average bond length ($2.399(4)$ Å) (Table 2) of Gd–O bonds in **1e** is slightly longer than that ($2.37(1)$ Å) of Gd–O (carbonyl oxygen) bonds in $[\text{Hg}_2(2\text{-oxazolidone})_4\text{Gd}$

Fig. 3. ORTEP drawing of $[\text{Eu}(\text{pu})_8](\text{OTf})_3$ (**1d**).

$(\text{NO}_3)_3]$.¹⁶ The average coordination bond ($2.389(4)$ Å) (Table 2) in the terbium complex (**1f**) is shorter than those of Tb–O (THF) bonds in $[\text{TbCl}_2(\text{thf})_5][\text{TbCl}_4(\text{thf})_2]$ ($2.40(2)$ Å) (cation) and ($2.344(3)$ Å) (anion),¹⁴ taking into account of the difference of the coordination number. The ionic radius of octa-coordinated terbium ion is 0.12 Å larger than that of hexa-coordinated terbium ion, and is 0.05 Å larger than that of hepta-coordinated terbium ion.⁷ The average bond distance ($2.400(4)$ Å) (Table 2) of Yb–O bonds in **1i** is almost the same as that ($2.271(4)$ Å) of Yb–O (carbonyl oxygen) bond in $\text{YbCl}_3(\varepsilon\text{-caprolactone})(\text{thf})_2$,¹⁴ but is shorter than that ($2.304(6)$ Å) of Yb–O (THF) bonds in $\text{YbCl}_3(\varepsilon\text{-caprolactone})(\text{thf})_2$, taking into account of the difference of the ionic radii (0.12 Å). The coordination bonds of **1i** are longer than those ($2.265(5)$ – $2.336(5)$ Å) of Yb–O bonds in $\{(\text{dmf})_{10}\text{Yb}_2[\text{Ni}(\text{CN})_4]_3\}_\infty$,¹⁷ and are longer than those of the dysprosium complex (**1g**) and the holmium complex (**1h**). These results mean that the coordination bonds in **1i** are longer than those expected from lanthanoid contraction. However, the major reason of the long coordination bonds of the ytterbium complex could not be clarified. As shown in Table 3, these average bond lengths of M–O (PU) in rare earth PU complexes are shorter than those of M–O (HMPA) in rare earth HMPA complexes, indicating that the coordination ability of PU ligand is weaker than that of HMPA ligand as mentioned above in complex **1a**.

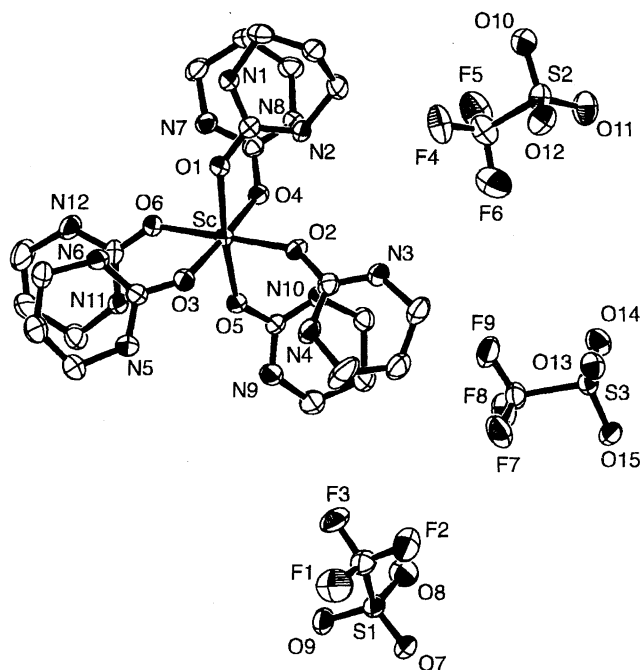
Previously we observed the tetrad effects in the coordination bonds in a series of HMPA coordinated lanthanide triflates.^{3c} In order to examine the tetrad effect on the coordination bonds in the lanthanide complexes bearing PU

Table 3. Comparison of Average Ln–O Bond Lengths between $[\text{M}(\text{pu})_6](\text{OTf})_3$ and $[\text{M}(\text{Otf})_2(\text{hmpa})_4]\text{OTf}\cdot\text{CHCl}_3$ ^{3c}

	$[\text{M}(\text{pu})_6](\text{OTf})_3$ M–O (PU) (Å)	$[\text{M}(\text{Otf})_2(\text{hmpa})_4]\text{OTf}\cdot\text{CHCl}_3$ M–O (HMPA) (Å)
Y–O	2.367(4)	2.194(3)
Nd–O	2.453(4)	2.293(4)
Sm–O	2.426(4)	2.259(5)
Eu–O	2.406(4)	2.248(4)
Gd–O	2.399(4)	2.238(4)
Tb–O	2.389(4)	2.220(4)
Dy–O	2.380(4)	2.204(4)
Ho–O	2.363(4)	2.200(4)
Yb–O	2.400(4)	2.158(4)

ligands, the respective Ln–O bond lengths have been plotted vs. atomic number as shown in Fig. 4. The tetrad effect was not observed in the coordination bonds, but lanthanoid contraction was observed except in the ytterbium complex. We consider that exact resemblance of the crystal structure containing positions of counter anions and crystal solvents is indispensable for emergence of the tetrad effect in the coordination bonds of the lanthanide complexes. In the HMPA coordinated lanthanide triflates, the molecular structures of these complexes (Ln = Ce–Lu) closely resembled each other, including the positions of non-coordinated triflate anion and chloroform.^{3c} In the present case, the structures around the central metals closely resemble each other; however, the positions of the three triflate anions are different from those of complex **1a**, as shown in Fig. 3. Owing to this fact, various hydrogen bonds were observed between the triflate anions and PU ligands. Therefore, the tetrad effect was not observed in the coordination bonds of these complexes.

$[\text{Sc}(\text{pu})_6](\text{OTf})_3$ (2). The reaction of anhydrous scandium triflate with 6 equiv of PU in methanol gave complex **2** quantitatively. The molecular structure of **2** was determined by X-ray structural analysis. The ORTEP drawing of complex **2** is shown in Fig. 5. The selected bond lengths

Fig. 5. Molecular structure of $[\text{Sc}(\text{pu})_6](\text{OTf})_3$ (**2**).

and angles are given in Table 4. The central scandium atom is hexa-coordinated by six PU molecules to form a trigonal antiprism structure. The ionic radius of the scandium atom is 0.2 Å smaller than that of the samarium atom;⁷ therefore, only six PU molecules coordinate to the scandium atom. The average bond distance (2.054(4) Å) between the scandium atom and the oxygen atoms of PU ligands is nearly equal to that (2.060(6) Å) of Sc–O (HMPA) in $[\text{Sc}(\text{Otf})_2(\text{hmpa})_4]\text{OTf}$.^{3c} Like complex **1a**, a pair of the ligands are interacting through hydrogen bonds such as O1...N7 (3.145(4) Å) and O4...N2 (3.282(5) Å). The hydrogen bonds such as O4...N10 (3.051(5) Å) among the adjacent ligands are also observed. The average bond angle of Sc–O–C (138.8(4)°) is nearly equal to that of complex **1a**. The three triflate anions

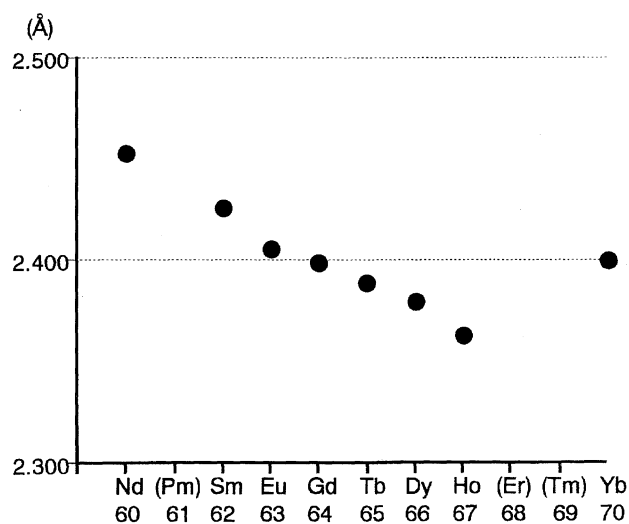


Fig. 4. Average Ln–O bond lengths vs. atomic number.

Table 4. Selected Bond Lengths (Å) and Angles (deg) for $[\text{Sc}(\text{pu})_6](\text{OTf})_3$ (**2**)

Sc–O(1)	2.046(3)	Sc–O(2)	2.044(4)
Sc–O(3)	2.040(3)	Sc–O(4)	2.075(3)
Sc–O(5)	2.062(4)	Sc–O(6)	2.056(4)
O(1)...N(7)	3.145(4)	O(2)...N(2)	2.979(5)
O(2)...N(10)	3.207(5)	O(3)...N(4)	3.440(6)
O(3)...N(11)	3.496(5)	O(4)...N(2)	3.282(5)
O(4)...N(10)	3.051(5)	O(5)...N(4)	3.469(6)
O(5)...N(11)	3.021(5)	O(6)...N(6)	3.179(5)
O(6)...N(7)	3.057(5)		
O(1)–Sc–O(2)	89.0(1)	O(1)–Sc–O(3)	95.1(1)
O(1)–Sc–O(4)	86.7(1)	O(1)–Sc–O(5)	171.9(1)
O(1)–Sc–O(6)	92.7(1)	O(2)–Sc–O(3)	94.3(1)
O(4)–Sc–O(5)	85.7(1)	O(4)–Sc–O(6)	87.1(1)
Sc–O(1)–C(1)	137.0(3)	Sc–O(2)–C(5)	145.2(4)
Sc–O(3)–C(9)	140.1(3)	Sc–O(4)–C(13)	134.2(3)
Sc–O(5)–C(17)	136.7(3)	Sc–O(6)–C(21)	139.6(3)

are not coordinated to the scandium atom, thus resulting in a tricationic complex.

[Sm(dmpu)₆](OTf)₃ (3). Anhydrous samarium(III) triflate reacted with 6 equiv of DMPU in THF to give a suspended solution. Removal of the solvent left a white powder, and the resultant complex was recrystallized from a THF solution. An X-ray structural analysis reveals the molecular structure of complex **3** as illustrated in Fig. 6. The selected bond lengths and angles are listed in Table 5. The samarium atom is coordinated by six DMPU ligands to form a hexa-coordinated octahedral structure. All the DMPU ligands coordinate perpendicularly to the samarium atom to avoid the steric repulsion of the methyl groups of DMPU. Like complexes **1a** and **2**, three triflate anions are not coordinated to the samarium atom. These results indicate that DMPU is a strong oxygen donor ligand.

In order to estimate the coordination ability of PU and DMPU, complex **3** is compared with complex **1a**. Both complexes are tricationic, and contain the same counter an-

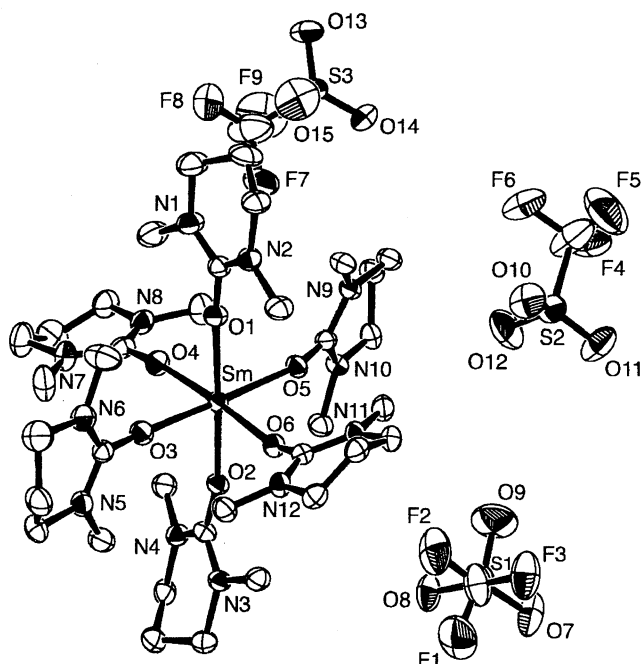


Fig. 6. ORTEP drawing of [Sm(dmpu)₆](OTf)₃ (**3**).

Table 5. Selected Bond Lengths (Å) and Angles (deg) for [Sm(dmpu)₆](OTf)₃ (**3**)

Sm–O(1)	2.304(7)	Sm–O(2)	2.312(6)
Sm–O(3)	2.282(7)	Sm–O(4)	2.298(7)
Sm–O(5)	2.338(6)	Sm–O(6)	2.311(6)
O(1)–Sm–O(2)	175.9(2)	O(1)–Sm–O(3)	89.0(3)
O(1)–Sm–O(4)	88.5(3)	O(1)–Sm–O(5)	87.3(2)
O(1)–Sm–O(6)	92.7(3)	O(3)–Sm–O(4)	88.9(3)
O(3)–Sm–O(5)	176.2(2)	O(3)–Sm–O(6)	87.6(2)
O(4)–Sm–O(5)	91.9(3)	O(5)–Sm–O(6)	91.7(2)
Sm–O(1)–C(1)	173.0(7)	Sm–O(2)–C(7)	161.4(6)
Sm–O(3)–C(13)	172.2(7)	Sm–O(4)–C(19)	172.4(7)
Sm–O(5)–C(25)	161.6(7)	Sm–O(6)–C(31)	162.6(7)

ions and the same metal ion. The major difference is the coordination number. The effective ionic radius of hexa-coordinated samarium complexes is 0.12 Å smaller than that of octa-coordinated samarium complexes by Shannon's ionic radii.⁷ Therefore, the average bond length (2.306(7) Å) of Sm–O (carbonyl oxygen) in complex **3** is nearly equal to that of complex **1a**, (2.436(4) Å), taking into account the difference in the effective ionic radii. These results indicate that PU and DMPU ligands possess similar electron-donating ability. The difference in the coordination number can be ascribed to the fact that the DMPU ligand is bulkier than the PU ligand.

[Sm(OTf)₂(dmi)₅](OTf) (4). Complex **4** was synthesized by the reaction of anhydrous samarium(III) triflate with 5 equiv of DMI in THF. The complex was recrystallized from a THF solution, and the molecular structure was determined by X-ray structural analysis, as shown in Fig. 7. The selected bond lengths and angles are summarized in Table 6. The central samarium atom is hepta-coordinated by five DMI molecules in the equatorial plane and two triflate anions in the trans position to form a distorted pentagonal bipyramidal structure. All DMI ligands in **4** are canted in propeller-like fashion around the metal center to avoid the steric repulsion of the methyl groups of the DMI ligands. The average bond length (2.350(6) Å) of Sm–O (DMI) is shorter than that of Sm–OTf (2.401(6) Å), indicating that the DMI ligands, although they are neutral ligands, coordinate to the samarium atom more strongly than the triflate anions. The other triflate anion is not coordinated to the samarium atom, thus forming a monocationic complex, whereas the complex **3** is tricationic, indicating that the coordination ability of the DMI ligand is

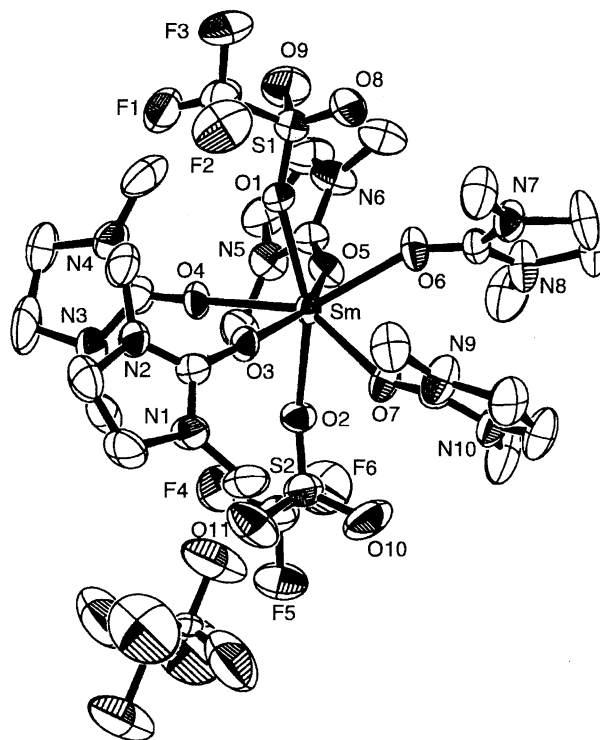


Fig. 7. ORTEP drawing of [Sm(OTf)₂(dmi)₅](OTf) (**4**).

Table 6. Selected Bond Lengths (Å) and Angles (deg) for [Sm(OTf)₂(dmi)₅]OTf (**4**)

Sm–O(1)	2.402(6)	Sm–O(2)	2.404(6)
Sm–O(3)	2.333(6)	Sm–O(4)	2.346(5)
Sm–O(5)	2.328(6)	Sm–O(6)	2.381(6)
Sm–O(7)	2.371(6)		
O(1)–Sm–O(2)	159.9(2)	O(1)–Sm–O(3)	81.7(3)
O(1)–Sm–O(4)	80.2(2)	O(1)–Sm–O(5)	94.2(3)
O(1)–Sm–O(6)	75.4(2)	O(1)–Sm–O(7)	121.8(2)
O(3)–Sm–O(4)	78.4(2)	O(3)–Sm–O(7)	77.0(2)
O(4)–Sm–O(5)	77.9(2)	O(5)–Sm–O(6)	77.8(2)
O(6)–Sm–O(7)	72.6(3)	Sm–O(3)–C(4)	154.2(6)
Sm–O(4)–C(9)	178.9(7)	Sm–O(5)–C(14)	154.6(6)
Sm–O(6)–C(19)	153.4(7)	Sm–O(7)–C(24)	153.7(7)

weaker than that of the DMPU ligand. The other monocationic samarium(III) triflate complex is [Sm(OTf)₂(hmpa)₄]-OTf·CHCl₃ (**5**) which forms a hexa-coordinated octahedral structure.^{3f} Four HMPA molecules are coordinated in the equatorial plane in the complex **5**. It can be considered that the five DMI molecules in **4** are able to coordinate to the samarium atom owing to the small bulk of DMI compared to that of HMPA.

In order to compare the coordination ability of DMI with that of HMPA, the coordination bonds of the two complexes **4** and **5** were compared. The average bond length (2.350(6) Å) of Sm–O (DMI) in **4** is apparently longer than that of Sm–O (HMPA) (2.259(4) Å) in **5**, although the ionic radius of hepta-coordinated samarium complexes is 0.06 Å larger than that of hexa-coordinated samarium complexes.⁹ These facts indicate that the coordination ability of DMI toward the samarium atom is weaker than that of HMPA. This consideration is also supported by the fact that the average bond length between the samarium atom and the oxygen atoms of four HMPAs in complex **5** is 0.1 Å shorter than that between the samarium atom and the oxygen atoms of two triflate anions, whereas the corresponding average coordination bond of DMI ligands in complex **4** is 0.05 Å shorter than that of triflate anions.

This work was supported by a Grant-in-Aid from Ministry of Education, Science, Sport and Culture, and by a "Research for the Future" program of the Japan Society for the Promotion of Science. We thank Central Glass Co., Ltd. for the gift of trifluoromethanesulfonic acid.

References

- Recent reviews of organic reactions promoted by lanthanide triflates see: a) S. Kobayashi, *Synlett*, **1994**, 689. b) S. Kobayashi, I. Hachiya, H. Ishitani, M. Moriwaki, and S. Nagayama, *Zh. Org. Khim.*, **32**, 214 (1996). c) L. Tonks and J. M. J. Williams, *Organomet. Chem.*, **26**, 180 (1998). d) S. Kobayashi, *Eur. J. Org. Chem.*, **1999**, 15.
- Lanthanide triflates-promoted organic reactions: a) J. H. Forsberg, V. T. Spaziano, T. M. Balasubramanian, G. K. Liu, S. A. Kinsley, C. A. Duckworth, J. J. Poteruca, P. S. Brown, and J. L. Miller, *J. Org. Chem.*, **52**, 1017 (1987). b) G. A. Molander, E. R.

- Burkhardt, and P. Weinig, *J. Org. Chem.*, **55**, 4990 (1990). c) S. Kobayashi and I. Hachiya, *Tetrahedron Lett.*, **33**, 1625 (1992). d) J. Inanaga, Y. Yokoyama, and T. Hanamoto, *Tetrahedron Lett.*, **34**, 2791 (1993). e) S. Kobayashi, *Synlett*, **1994**, 689. f) S. Kobayashi and I. Hachiya, *J. Org. Chem.*, **59**, 3590 (1994). g) S. Kobayashi and H. Ishitani, *J. Am. Chem. Soc.*, **116**, 4083 (1994). h) M. P. Sibi and J. Ji, *Angew. Chem., Int. Ed. Engl.*, **35**, 190 (1996). i) T. Hanamoto, Y. Sugimoto, Y. Yokoyama, and J. Inanaga, *J. Org. Chem.*, **61**, 4491 (1996). j) S. Kobayashi and S. Nagayama, *J. Am. Chem. Soc.*, **119**, 10049 (1997). k) S. Kobayashi and S. Nagayama, *J. Am. Chem. Soc.*, **120**, 2985 (1998). l) B. H. Lipshutz, J. A. Sclatani, and T. Takanami, *J. Am. Chem. Soc.*, **120**, 4021 (1998). m) S. Kobayashi and S. Nagayama, *J. Am. Chem. Soc.*, **120**, 4554 (1998).

- Some lanthanide triflate complexes have been structurally characterized by X-Ray crystallographic analyses: a) J. M. Harrowfield, D. L. Kepert, J. M. Patrick, and A. H. White, *Aust. J. Chem.*, **36**, 483 (1983). b) P. H. Smith and K. H. Raymond, *Inorg. Chem.*, **24**, 3469 (1985). c) C. B. Castellani, O. Carugo, M. Giustil, and N. Sardone, *Eur. J. Solid State Inorg. Chem.*, **32**, 1089 (1995). d) J. Chen, Y. Zhang, X. Zheng, A. Vij, D. Wingate, D. Meng, K. White, R. L. Kirchmeier, and J. M. Shreeve, *Inorg. Chem.*, **35**, 1590 (1996). e) T. Imamoto, M. Nishiura, Y. Yamanoi, H. Tsuruta, and K. Yamaguchi, *Chem. Lett.*, **1996**, 875. f) M. Nishiura, Y. Yamanoi, H. Tsuruta, K. Yamaguchi, and T. Imamoto, *Bull. Soc. Chim. Fr.*, **134**, 411 (1997). g) R. S. Dickins, J. A. Howard, C. W. Lehmann, J. Moloney, D. Parker, and R. D. Peacock, *Angew. Chem., Int. Ed. Engl.*, **36**, 521 (1997). h) H. A. Alvarez, J. R. Matos, P. C. Isolani, G. Vicentini, E. E. Castellano, and J. Zukerman-Schpector, *J. Coord. Chem.*, **43**, 349 (1998). i) H. C. Aspinall, N. Greeves, and E. G. McIver, *J. Alloys Compd.*, **1998**, 773. j) K. Mikami, O. Kotera, Y. Motoyama, and M. Tanaka, *Inorg. Chem. Commun.*, **1**, 10 (1998).

- A few of the urea derivatives coordinated lanthanide complexes were synthesized. a) A. Seminara, A. Musumeci, and A. Chisari, *J. Inorg. Nucl. Chem.*, **40**, 269 (1978). b) S. Calogero, A. Seminara, and U. Russo, *Gazz. Chim. Ital.*, **109**, 45 (1979). c) G. Vicentini and L. B. Zinner, *J. Inorg. Nucl. Chem.*, **42**, 1510 (1980). d) K. Mikami, O. Kotera, Y. Motoyama, and M. Tanaka, *Inorg. Chem. Commun.*, **1**, 10 (1998).

- Z. Hou, A. Fujita, Y. Zhang, T. Miyano, H. Yamazaki, and Y. Wakatsuki, *J. Am. Chem. Soc.*, **120**, 754 (1998).

- Z. Xie, K. Chui, Q. Yang, T. C. W. Mak, and J. Sun, *Organometallics*, **17**, 3937 (1998).

- R. D. Shannon, *Acta Crystallogr., Sect. A*, **A32**, 751 (1976).

- D. C. Bradley, J. S. Ghotra, F. A. Hart, M. B. Hursthouse, and P. R. Raithby, *J. Chem. Soc., Dalton Trans.*, **1977**, 1166.

- W. J. Evans, J. W. Grate, and R. J. Doedens, *J. Am. Chem. Soc.*, **107**, 1671 (1985).

- W. J. Evans, J. L. Shreeve, and R. J. Doedens, *Inorg. Chem.*, **32**, 245 (1993).

- D. M. L. Goodgame, S. P. W. Hill, A. M. Smith, and D. J. Williams, *J. Chem. Soc., Dalton Trans.*, **1994**, 859.

- A. A. Kapshuk, V. M. Amirkhanov, V. V. Spopenko, and V. S. Fundamenskii, *Ukr. Khim. Zh.*, **53**, 227 (1987).

- S. W. A. Bligh, N. Choi, H. R. Hudson, C. M. McGrath, and M. McPartlin, *J. Chem. Soc., Dalton Trans.*, **1994**, 2335.

- W. J. Evans, J. L. Shreeve, J. W. Ziller, and R. J. Doedens, *Inorg. Chem.*, **34**, 576 (1995).

- J. Liu, E. A. Meyers, J. A. Cowan, and S. G. Shore, *Chem. Commun.*, **1998**, 2043.

- L. H. Carrad, D. M. L. Goodgame, S. P. W. Hill, and D. J. Williams, *J. Chem. Soc., Dalton Trans.*, **1993**, 1003.

- D. W. Knochle and S. G. Shore, *Inorg. Chem.*, **35**, 1747

(1996).

18 F. Hai-Fu, "SAPI91, Structure Analysis Program with Intelligent Control," Rigaku Corporation, Tokyo, Japan (1991).

19 A. Altomare, M. C. Burla, M. Camalli, M. Cascarano, C. Giacovazzo, A. Guagliardi, and G. Polidori, "SIR92, Program for the Solution of Crystal Structure," 1994.
